Prediction of Microstructure Evolution and Hardness Distribution in the Weld Repair of Carbon Steel Pipeline

V. Li and D. Kim

Abstract

This article presents an integrated modeling approach for coupled analysis of heat transfer and microstructure evolution in welding carbon steel. The modeling procedure utilizes commercial finite element code ABAQUS/Standard as the platform for solving the equation of heat conduction. User subroutines that implement computational thermodynamics and kinetics models are integrated with the FEA code to compute the transient microstructure evolution. In this study, the integrated models are applied to simulate the hot-tap repair welding of carbon steel pipeline. Microstructural components are treated as user output variables. Based on the predicted microstructure and cooling rates, hardness distributions in the welds were also predicted. The predicted microstructure and hardness distribution were found in good agreement with metallographic examinations and hardness measurements. This study demonstrates the applicability of computational models for the development of welding procedure for in-service pipeline repair.

Key Words : Weld process simulation, Microstructure evolution, Finite element analysis, Hot-tap welding, Repair welding.

1. Introduction

Weld repair of piping systems and pipelines in the United States is often required to be conducted in service and with pressurized fluids inside. Such weld repair process is commonly referred to as hot-tap welding. To date, hot-tap welding repair procedures have been developed primarily in the laboratories with same grade materials and similar part geometry and joint configurations. Weld repair procedures may be used for actual repairs once they prove that the welds can meet the requirements of mechanical properties per regulatory codes and standards. In addition to the requirements of other regulatory codes, the National Association of Corrosion Engineers International (NACE) dictates that that the maximum hardness in the weld heat-affected zone should not exceed 22 HRC (about 248 Hv) if a weld will be subjected to sulfide stress corrosion environment [1]. Recent development of weld modeling technology provides a predictive tool to expedite the development of repair welding procedure and to optimize welding procedures to meet the requirement of microstructure and hardness.

Controlled deposition welding techniques are widely used in the development of weld repair procedures. They involve intelligent manipulations of welding heat inputs between deposit layers to maximize the benefits of grain refinement in the heat-affected zone. This paper presents a coupled thermal-metallurgical modeling approach for the prediction of microstructure evolution and hardness distributions in the hot-tap repair welds of carbon steel that utilizes controlled deposition techniques. The objective of this study is to simulate the heat transfer, microstructure and hardness distribution in the repair welds. The feasibility of using computational model to assist the development and optimization of weld repair procedure will also be evaluated.

2. Materials and welding

The chemistry of the base metal plates and filler metal are presented in Table 1. Both the test plate and sleeve plate are 0.5 inch thick and are of ASTM A516 Grade 70 carbon steel. The compositions of the steels satisfy the chemical requirements of ASTM A516-90.

The work presented in this article involves the simulation of the fillet welds that join the sleeve to the runpipe or the patch plate to the test plate. The joint configuration is shown in Fig. 1. Before the welding,

V. Li : Department of Mechanical Engineering, Portland State University, Portland, U.S.A.
E-mail : victorli@cecs.pdx.edu
D. Kim : Westhollow Technology Center, Houston, U.S.A.
E-mail : dskim@equilontech.com

Table 1 Chemical composition of materials (wt.%)

Material	C	Mn	Si	Ni	Cr	Mo	Cu	V	Nb	Al	Ti
Base Plate	0.157	0.72	0.055	0.144	0.064	0.010	0.042	<0.004	<0.003	0.065	<0.001
Sleeve Plate	0.149	0.73	0.055	0.145	0.066	0.011	0.042	<0.004	<0.003	0.066	<0.001
Weld Metal	0.105	0.347	0.012	0.011	0.008	0.513	0.001	0.014	0.004	0.001	0.009

Table 2 Welding parameters

	GTAW	SMAW	
Filler Metal	AWS ER 70S-2	AWS E7018	AWS E7018
Size of filler Metal	1/8"	3/32"	1/8"
Current (A)	70 – 95	70 – 75	120 – 125
Voltage (V)	8 – 12	20 – 24	20 – 24

Fig. 1 Fillet weld joint configuration

the plates are preheated to 300 °F (422 K). Welding parameters used in the weld repair are listed in Table 2. The root pass is made with gas tungsten arc welding (GTAW). Other passes are made with shield metal arc welding (SMAW). During the welding operation, the inter-pass temperature is controlled below 450 °F (505 K). The welding current and voltage used in the weld repair fall into the normal operation range per the sizes of the electrodes.

3. Computational models

The repair weld design requires that each leg of the fillet weld be at least 3/8 inch (9.5 mm), which translate 45.4 mm^2 cross section area of the fillet weld joint. Once the electrodes are selected, the welding current and arc voltage are typically determined. The welding engineer can control the welding heat input by controlling the welding speed. In the design of weld repair, the welding travel speed can be estimated using the empirical relation between welding heat input and the cross-sectional area of weld deposit made with electrode E7018[2].

$$A(in^2) = 8.754 \times 10^{-4} Q(kJ/in) - 3.556 \times 10^{-3} \quad (1)$$

In this relation, A is the cross-sectional area of the weld in square inch and Q is the heat input in kJ/in. The estimated travel speed for the weld passes is 1.7 mm/sec in the fillet joint.

A two-dimensional finite element model (mesh) is developed for the simulation of the fillet welds, shown in Fig. 2. ABAQUS/CAE is used for the mesh generation. The elements are two-dimensional four-node quadrilateral linear elements. The finite element model has 3,157 nodes and 3,011 elements.

All the nodes in the model are assigned with an initial temperature of 373 K, which accounts for the effect of 100°C preheating. All free surfaces are subjected to natural convection with the ambient temperature of 298 K (25°C) that represents the boundary conditions in the laboratory welding conditions. The heat input from each welding arc is simulated with body heat flux into the element set that represents the weld deposit. The body heat flux is assumed to the uniform across the sectional area at any instant in time. Along the welding direction, the heat flux is assumed to satisfy Gauss distribution. The heat source model is implemented in the user subroutine DFLUX.

Element "birth-and-death" control techniques are used to account for the addition of weld deposit. Essentially, all the weld deposit passes are included in the original finite element model. Elements associated with weld passes to be deposited are deactivated first. Deactivated elements are re-activated at proper time during the simulation.

The mass density of the materials in the heat-transfer analyses remains constant at their room-temperature values, 7830 kg/m^3 for both the base metal plate and the weld metal. Typical temperature-dependent thermal conductivity and specific heat of low-carbon steel is used in the heat-transfer analysis for the base metal plate and

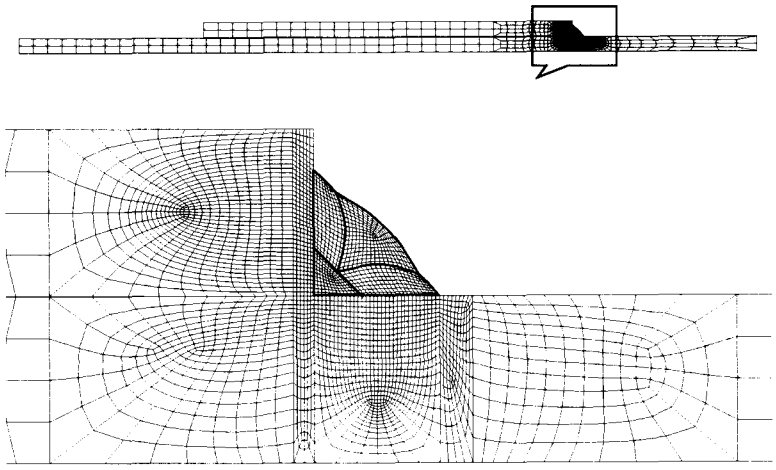

Fig. 2 Finite element model for the welded joint

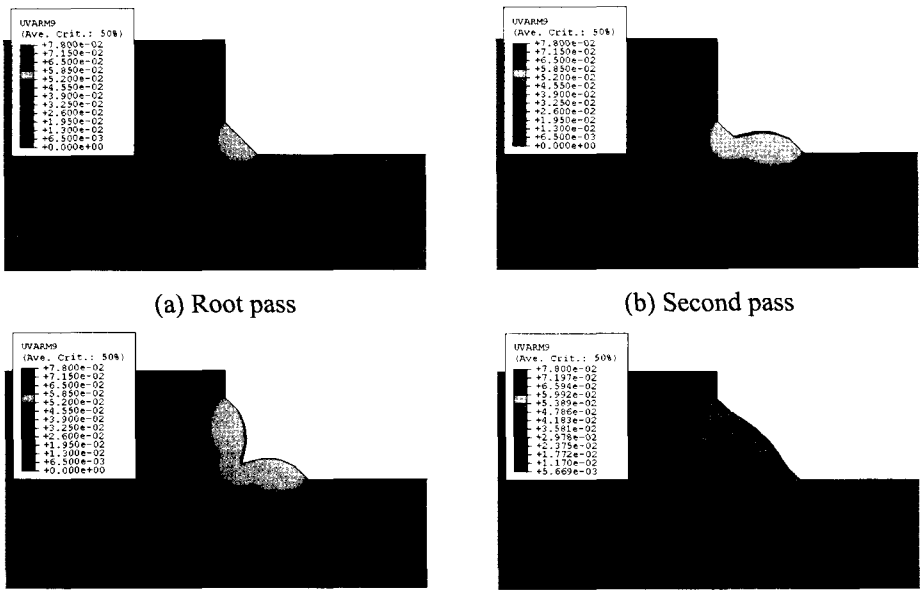

(a) Root pass (b) Second pass

(c) Third pass (d) Forth pass

Fig. 3 Prior austenite grain size (mm) in the fillet welds

the weld metal.

The theory, mathematical formulation, and numerical implementations of the models for phase transformations in steel subjected to arbitrary thermal cycles have been presented previously[3,4]. The microstructural models used in this study perform the following four major functions: characterization of the thermodynamics systems of the materials, computing growth of prior austenite grains, predicting phase transformations, and calculating the micro-hardness. To compute the microstructural evolution within the platform of ABAQUS/Standard, the microstructural models are integrated with ABAQUS / Standard solver in the form of a user subroutine UVARM. Subroutine UVARM is called at the end of each time increment when converged thermal solutions have been obtained. Within the user subroutine UVARM, the instantaneous temperature and temperature gradients at the element integration points can be accessed. The volume fractions of such microstructural constituents as ferrite, pearlite, bainite, martensite, austenite, etc. are defined as user defined output variables that are computed and updated. These output variables are saved into the result and output files for post-processing.

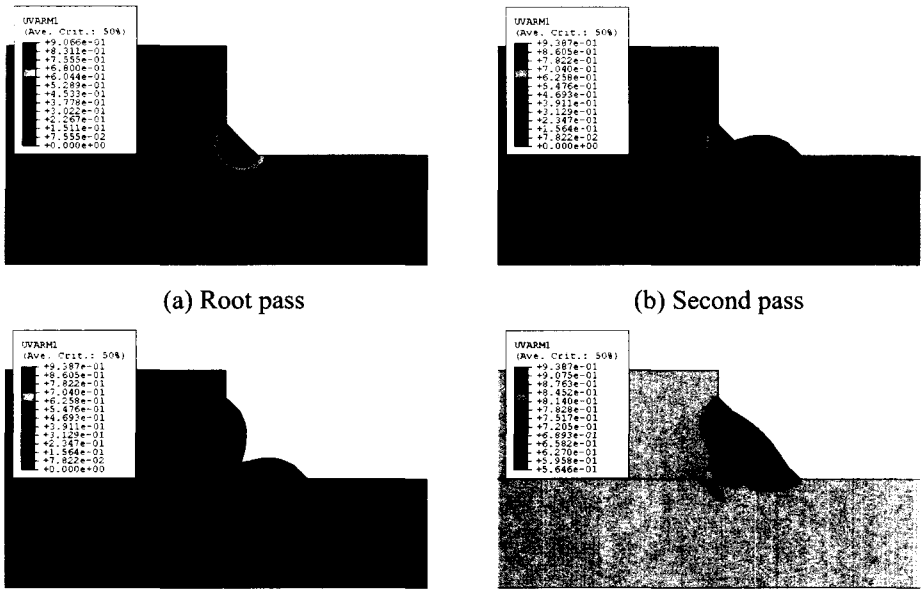

(a) Root pass (b) Second pass

(c) Third pass (d) Forth pass

Fig. 4 Predicted volume fraction of ferrite in the fillet welds

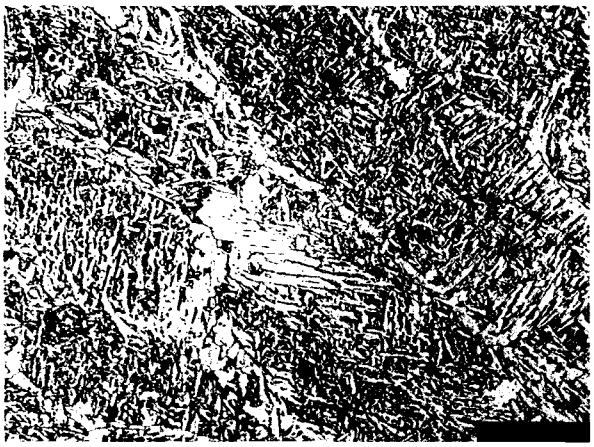

Fig. 5 Microstructure in the as-welded fusion zone

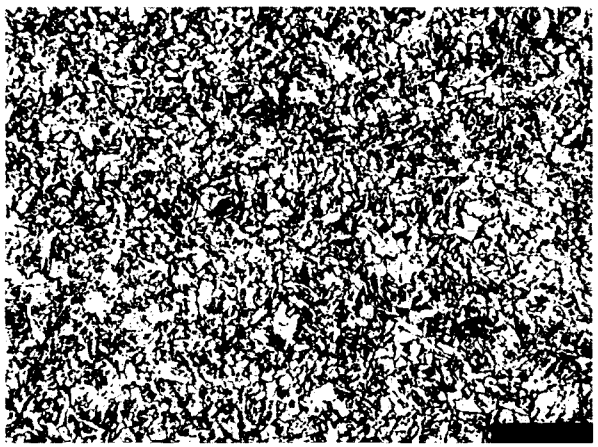

Fig. 6 Microstructure in the re-heated weld metal

4. Results and discussion

The predicted pass-by-pass changes of prior austenite grain sizes are presented in Fig. 3. Note that there is a thin layer of coarse grain region adjacent to the weld fusion line in the heat-affected zone of base metal adjacent to the fusion zone. Subsequent weld passes do not completely refine the gain sizes of this region.

The predicted amounts of pearlite in the weld heat-affected zone and fusion zone are negligible. The predicted microstructure in the weld fusion zone is predominately ferrite, as shown in Fig. 4. The coarse grain heat-affected zone of the root pass in the base metal plates consist of roughly 80% bainite, 10% martensite, and 10% ferrite. This region is heated up to austenite region by subsequent weld passes and the austenite transforms to primarily ferrite and bainite during the cooling. There is about 42% bainite remain in this region after the completion of all welding passes. Note that subsequent passes did not completely refine the grain size of prior austenite in the heat-affected zone of the base metal plates. The microstructural changes in the re-heated heat affected zone of base metal are attributed to the higher heat input and slower cooling rates in the

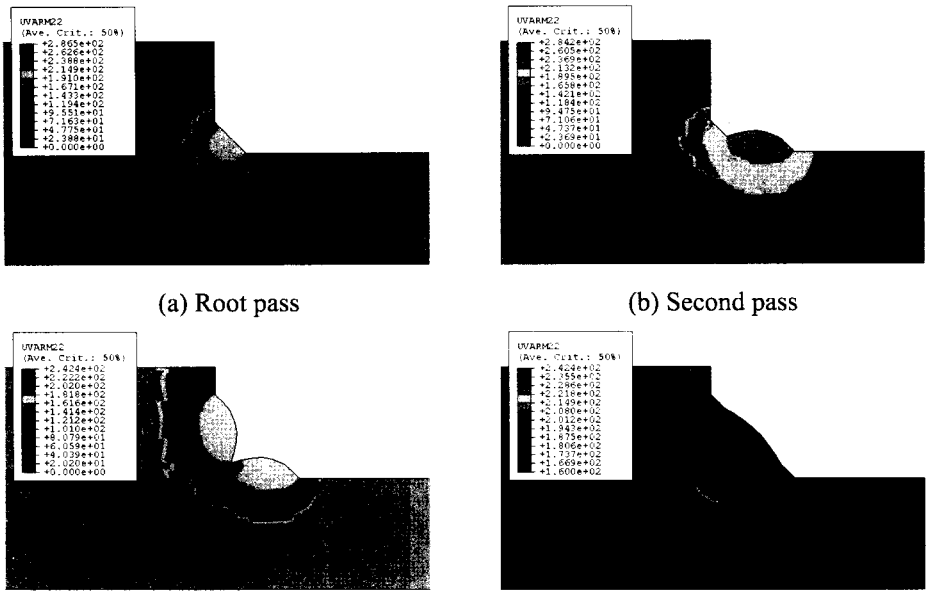

(a) Root pass (b) Second pass

(c) Third pass (d) Forth pass

Fig. 7 Hardness (HV) distribution in the fillet welds

subsequent welding passes. Also, note that no computation models make no distinctions of different ferrite morphologies.

Fig. 5 shows the microstructure in the as-welded fusion zone. It consists of various morphologies of ferrite, namely, primary ferrite, ferrite with aligned carbides, and acicular ferrite per IIW terminology [5]. A portion of the weld deposit is re-heated by the subsequent weld passes to austenite region. Primary ferrite is formed in this region upon cooling. The microstructure in the re-heated weld metal is shown in Fig. 6.

The predicted hardness distributions after each weld pass are presented in Fig. 7. Only 10% martensite is formed in the coarse grain HAZ of the root pass. Yet, the predicted hardness has reached 287 HV, which exceeds the maximum hardness required by the NACE standard. However, the martensite was later transformed into austenite and ferrite. The final hardness values in the weld heat-affected zone do not exceed the 248 HV, which meet the hardness requirement of NACE standard[1]. The predicted hardness distributions in the fillet welds are found in good agreement with the experimental measurements. The original coarse grain heat-affected zone of the root pass has the highest hardness values, which is attributed to the formation of bainite in comparison with ferrite in the weld metal and heat affected zone in other locations.

The key challenge in developing proper repair welding procedure to meet the hardness requirement is to prevent the formation of martensite in the heat affected zone of base metal plates. The hardness difference between bainite and ferrite is moderate, not sufficient to cause the hardness exceeding the NACE standard. This study demonstrates that computational models which couple the heat transfer and metallurgical reactions can be readily used to assist the development of repair welding procedure. Trial procedures can be easily simulated and evaluated

5. Conclusion

Integrated computational models are used in this study to predict the heat transfer, microstructure evolution, and resultant hardness distribution in the hot-tap repair welds of carbon steel. The predicted microstructure and hardness distribution are in good agreement with metallographic examinations and hardness measurements. The results from the analyses suggest that the current repair welding procedure will meet the maximum hardness requirement per NACE standard. This study also demonstrates the feasibility of utilizing computational modeling techniques to assist the development of repair welding procedures.

References

1. NACE Standard MR 0175-2002 : Sulfide Stress Cracking Resistant Metallic Materials for Oilfield Equipment
2. T. A . Bubenik, R. D. Fischer, G. R. Whitacre, D. J. Jones, J. F. Kiefner, M. Cola and W. A. Bruce : Final Report on Investigation and Prediction of Cooling Rates during Pipeline Maintenance Welding, *American Petroleum Institute*, December (1991)
3. M. V. Li : Computational Modeling of Heat Transfer and Microstructure Development in the Electroslag Cladding Heat-Affected Zone of Low-Alloy Steels, Ph. D. Dissertation, Oregon Graduate Institute of Science and Technology , January (1996)
4. M. V. Li, D. V. Niebuhr, L. L. Meekisho and D. G. Atteridge : A Computational Model for the Prediction of Steel Hardenability, *Metallurgical Transactions B*, Vol. 29B, No. 3 (1998), pp. 661-672
5. S. A. Gedeon : Resistance Spot Welding of Galvanized Steel Sheet, M.S. Thesis, Massachusetts Institute of Technology, (1984)
6. Guide to the Light Microscope Examination of Ferritic Steel Weld Metals, *IIW Doc. No. IX-1533-88, IXJ-123-87*, June (1988)